Neuron, Vol. 38, 965–976, June 19, 2003, Copyright ©2003 by Cell Press

Enhanced Learning and Memory in Mice Lacking Na^+/Ca^{2+} Exchanger 2

Daejong Jeon,[1] Yu-Mi Yang,[2] Myung-Jin Jeong,[1] Kenneth D. Philipson,[3] Hyewhon Rhim,[2] and Hee-Sup Shin[1,*]

[1]National Creative Research Initiative Center for Calcium & Learning
[2]Center for Medical Science Research
Korea Institute of Science and Technology
Seoul, 136-791
Korea
[3]Cardiovascular Research Laboratories
MRL 3-645
UCLA School of Medicine
Los Angeles, California 90095

Summary

The plasma membrane Na^+/Ca^{2+} exchanger (NCX) plays a role in regulation of intracellular Ca^{2+} concentration via the forward mode (Ca^{2+} efflux) or the reverse mode (Ca^{2+} influx). To define the physiological function of the exchanger in vivo, we generated mice deficient for NCX2, the major isoform in the brain. Mutant hippocampal neurons exhibited a significantly delayed clearance of elevated Ca^{2+} following depolarization. The frequency threshold for LTP and LTD in the hippocampal CA1 region was shifted to a lowered frequency in the mutant mice, thereby favoring LTP. Behaviorally, the mutant mice exhibited enhanced performance in several hippocampus-dependent learning and memory tasks. These results demonstrate that NCX2 can be a temporal regulator of Ca^{2+} homeostasis and as such is essential for the control of synaptic plasticity and cognition.

Introduction

The major cellular function of the Na^+/Ca^{2+} exchanger (NCX) is to exchange electrogenically one Ca^{2+} for three Na^+, depending on the electrochemical gradients across the plasma membrane. Normally the NCX serves as a Ca^{2+} extrusion mechanism driven by the Na^+ electrochemical gradient. However, it has also been shown that Ca^{2+} influx through the NCX can occur under certain conditions (Hryshko and Philipson, 1997; Blaustein and Lederer, 1999). Despite the importance of Ca^{2+} homeostasis, the physiological role of NCX in the brain is not well understood.

Both NCX and the plasma membrane Ca^{2+}-ATPase (PMCA) play a central role in controlling the resting level of intracellular Ca^{2+} ($[Ca^{2+}]_i$) in excitable cells such as neurons and cardiac myocytes. PMCA binds Ca^{2+} with a high affinity but with a relatively low turnover rate (i.e., the amount of Ca^{2+} transported per carrier per unit time, typically $\sim$100 s^{-1}). In contrast, NCX has about a 10-fold lower affinity but a 10- to 50-fold higher turnover rate for Ca^{2+} compared to PMCA. Under the circumstances of cell activation and a substantial elevation of $[Ca^{2+}]_i$, PMCA may be saturated with Ca^{2+} and its capacity to extrude Ca^{2+} rapidly may be limited, while the NCX may play a dominant role in this process (Sanchez-Armass and Blaustein, 1987; Blaustein and Lederer, 1999).

Three different isoforms of NCX (NCX1, NCX2, NCX3) are encoded by distinct genes in mammals (Nicoll et al., 1990, 1996; Li et al., 1994). They share similar biophysical properties (Linck et al., 1998; Blaustein and Lederer, 1999) but exhibit differences in expression during development and in adults. NCX2 transcripts are predominant in adult brains (Sakaue et al., 2000; Gibney et al., 2002; Yu and Colvin, 1997).

The contribution of NCX to clearance of intracellular Ca^{2+} was demonstrated in parallel fibers (Regehr, 1997) and Purkinje cells (Fierro et al., 1998) of the cerebellum. In another study, an administration of antisense oligodeoxynucleotide to a conserved region of the three NCX isoforms resulted in a slower return to baseline Ca^{2+} levels following activation of Ca^{2+} influx by NMDA (Ranciat-McComb et al., 2000).

NCX has also been shown to play a major role in the regulation of $[Ca^{2+}]_i$ in synaptic sites of hippocampal neurons and to influence synaptic vesicle recycling (Reuter and Porzig, 1995; Bouron and Reuter, 1996). Thus, blocking NCX function by replacement of extracellular Na^+ with Li^+ increased $[Ca^{2+}]_i$ during and after stimulation in nerve terminals, resulting in faster initial rates of exocytosis of synaptic vesicles. Fast and prolonged increase in $[Ca^{2+}]_i$ in postsynaptic neurons may result from a combination of increased neurotransmitter release from presynaptic terminals and delayed Ca^{2+} clearance in postsynaptic sites. Therefore, the delayed Ca^{2+} clearance may enforce synaptic activity both by pre- and postsynaptic mechanisms. Nevertheless, no studies have been reported that examined the role of NCX in the regulation of synaptic plasticity.

Although many studies have concentrated on Ca^{2+} influx through membrane channels or Ca^{2+} release from internal Ca^{2+} stores, the contributions of Ca^{2+} clearance in the plasma membrane have often been overlooked in studies of synaptic plasticity. To address these issues, we generated a null mutation of the *NCX2* gene, which is the major isoform in the brain. We analyzed the NCX2-deficient mice with respect to the regulation of $[Ca^{2+}]_i$ in neurons, the status of synaptic activities, and their capacity for learning and memory. The results provide conclusive evidence to support a critical role of NCX2 in hippocampal functions.

Results

Generation of NCX2 Knockout Mice

The targeting vector was constructed as described in Experimental Procedures. The wild-type locus, targeting vector, and disrupted locus are shown schematically in Figure 1A. Southern blot analysis of *Eco*RI-digested genomic DNA with the flanking probe demonstrated a

*Correspondence: shin@kist.re.kr

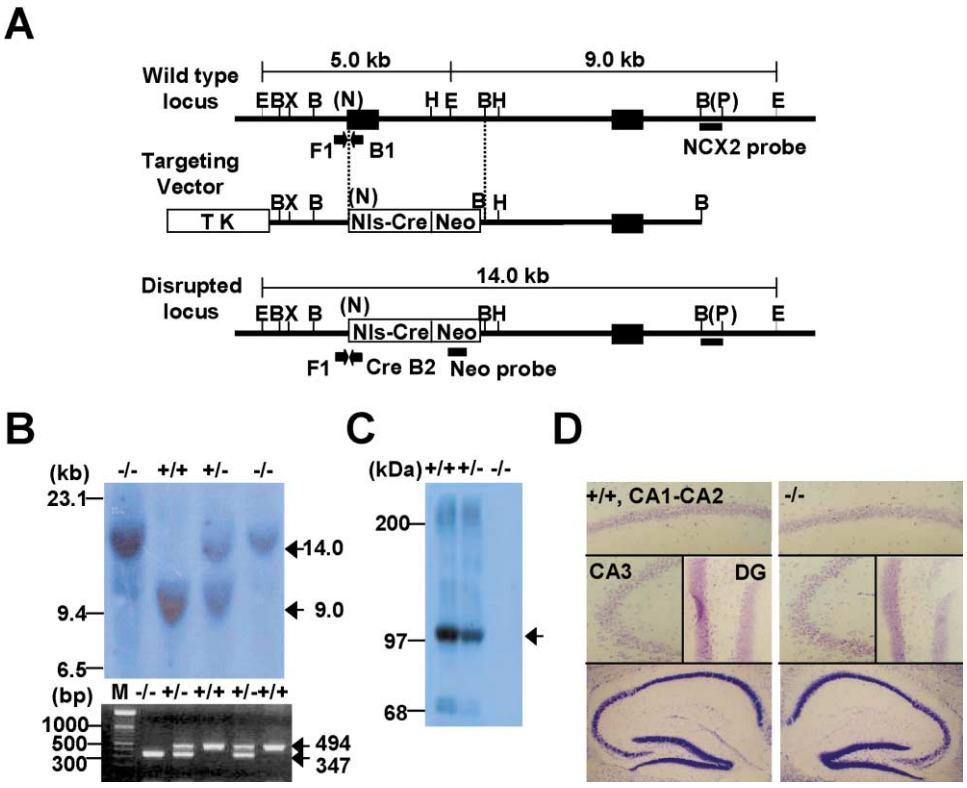

Figure 1. Gene Targeting of the NCX2 Locus

(A) Targeting strategy of NCX2 locus. Symbols: black box, the targeted exon (exon1 and 2, in order); horizontal arrowheads, the position of the PCR primers; black bar underneath the wild-type and disrupted locus, the probe for Southern analysis; Nls, nuclear localization sequence; Cre, Cre recombinase; Neo, the NEO cassette; TK, the TK cassette; B, *Bam*HI; E, *Eco*RI; H, *Hind*III; N, *Nco* I; P, *Pst* I; X, *Xho* I.

(B) Southern blot and PCR analysis for genotyping. Top: tail tip genomic DNAs were digested with *Eco*RI and hybridized with the NCX2 probe. The 9.0 kb segment corresponds to the wild allele; the 14.0 kb, the targeted allele. Bottom: the 494 bp band (F1, B1 primers), the PCR product of the wild-type allele; the 347 bp band (F1, Cre B2 primers), the product of the targeted allele. Molecular size makers are indicated on the left.

(C) Western blot analysis of membrane fractions of the wild-type, the NCX2$^{+/-}$, and the NCX2$^{-/-}$ whole brain. Arrowhead, estimated size of NCX2 protein.

(D) Normal gross morphology of the hippocampus of NCX2 mutant mouse. Coronal brain sections (8 μm) of mice at the age of 7 weeks were stained with cresyl violet. Images are at 100× (upper) and 40× (lower) original magnification.

targeted integration (Figure 1B). Western blot analysis demonstrated that NCX2 protein was not produced in the NCX2 mutant brain, thereby indicating that the gene targeting resulted in a null mutation for this locus (Figure 1C).

The NCX2 mutant mice exhibited normal growth and all major cytoarchitectonic divisions in the brain were unchanged. Cresyl violet staining of the coronal brain sections revealed no gross abnormalities in the hippocampus (Figure 1D).

NCX2 Expression Is Restricted to CNS

NCX2 was reported to be expressed only in brain and skeletal muscle (Li et al., 1994), although the skeletal muscle expression of NCX2 is controversial (Nicoll et al., 1996). We used RT-PCR to analyze tissue expression of NCX2 and found no evidence of NCX2 expression in skeletal muscle (Figure 2A). Furthermore, our extensive analysis demonstrated that the expression of NCX2 is restricted to CNS, brain, and spinal cord (Figure 2B).

In the absence of good antisera against NCX2 proteins that can be used for immunohistochemistry, we examined the expression pattern of NCX2 in the brain by using the expression of the Cre recombinase from the targeted locus. In Northern blot analysis of total brain RNA, an approximately 1.67 kb transcript of Cre recombinase was detected (Figure 2C). The NCX2 mutant mice were then crossed with the CAG-CAT-Z reporter mice (Sakai and Miyazaki, 1997). X-gal staining of the brain sections of these double transgenic mice (NCX2$^{+/-}$-CAG-CAT-Z) revealed expression throughout brain regions, with intense staining evident in the hippocampus (CA1, CA2, CA3, DG), cerebellum (granule, Purkinje), and cortex (Figure 2D).

Reduced Total Plasma Membrane NCX Currents in the Mutant Neurons

To examine the functional loss of the NCX2 current (I_{NCX}), the forward exchange currents (Ca^{2+} out/Na^{+} in) were measured by means of whole-cell patch-clamp recording in the CA1 pyramidal neurons of hippocampal slices as described in Experimental Procedures. I_{NCX} was activated by replacing the Li^{+} external buffer with a buffer containing 124 mM Na^{+} via perfusion. The peak

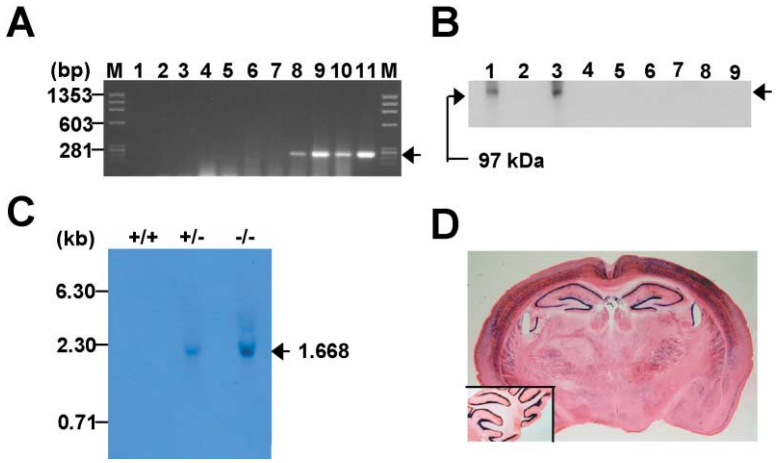

Figure 2. Tissue Distribution of NCX2

(A) RT-PCR showing NCX2 expression (255 bp) in extracts from brain and skeletal muscle of wild-type mice. No expression was detected in skeletal muscle as well as negative controls. Lane 1, water; 2, DNase-treated RNA from skeletal muscle of 1 day pup; 3, DNase-treated RNA from skeletal muscle of 6 weeks adult; 4, DNase-treated RNA from brain of 1 day pup; 5, DNase-treated RNA from brain of 6 weeks adult; 6, cDNA of skeletal muscle of 1 day pup; 7, cDNA of skeletal muscle of 6 weeks adult; 8, cDNA of brain of 1 day pup; 9, cDNA of brain of 3 weeks adult; 10, cDNA of brain of 6 weeks adult; 11, genomic DNA. Molecular size makers are indicated on the left.

(B) Western blot analysis of membrane fractions of 5-week-old wild-type tissues. Lane 1, spinal cord; 2, heart; 3, brain; 4, lung; 5, liver; 6, kidney; 7, pancreas; 8, spleen; 9, skeletal muscle. Note no signal in skeletal muscle. Arrowhead (right), estimated size of NCX2 protein.

(C) Northern blot analysis showing Cre recombinase expression in wild-type littermate, NCX2$^{+/-}$ and NCX2$^{-/-}$. Arrowhead, estimated size of Cre recombinase RNA.

(D) X-gal staining of a coronal brain section from a NCX 2$^{+/-}$-CAG-CAT-Z mouse. Inset: a brain section of cerebellum. Images are at 40× (inset) and 1.5× original magnification.

amplitude of the current was reduced in the mutant by approximately 50% compared to that in the wild-type (+/+, −193.39 ± 21.86 pA, n = 8; −/−, −84.45 ± 13.19 pA, n = 6, $p < 0.01$, Student's t test; Figure 3A). This demonstrates that NCX2 contributes significantly to the I_{NCX} in the CA1 pyramidal neurons while other NCX isoforms might support the remaining currents.

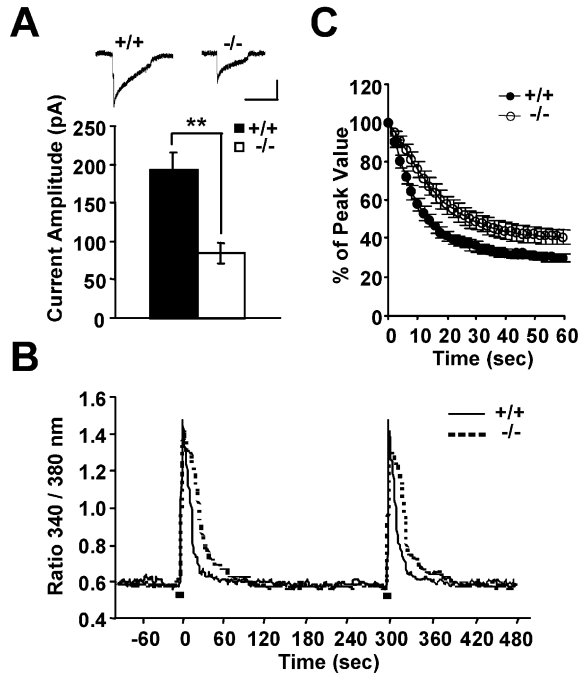

Figure 3. Reduced Total NCX Currents and Intracellular Ca^{2+} Measurement

(A) The forward exchange current (top). Current amplitude (bottom) at a holding potential of −40 mV in wild-type (8 slices, 5 mice) and mutant (6 slices, 4 mice). **$p < 0.01$, Student's t test. Scale bars equal 50 pA and 10 s.

(B) Glutamate-induced $[Ca^{2+}]_i$ changes in wild-type (continuous line) and mutant (dotted line). Scale bar equals 10 s, glutamate.

(C) $[Ca^{2+}]_i$ decay kinetics. Percent decrease from the peak of glutamate-induced $[Ca^{2+}]_i$ changes for 60 s following washing with normal buffer in wild-type (16 cells, 4 mice) and mutant (17 cells, 4 mice).

Delayed Ca^{2+} Clearance from the Mutant Neuronal Cells

To examine the effect on the $[Ca^{2+}]_i$ homoeostasis of the reduced I_{NCX} in the mutant hippocampal pyramidal neurons, we utilized the Ca^{2+} imaging analysis system using the fura-2 dye indicator as described in Experimental Procedures. Glutamate triggered a sharp increase in $[Ca^{2+}]_i$ in the cell bodies of CA1 pyramidal neurons followed by an initially rapid then slow recovery to the basal level (Figure 3B) as has been reported previously (Kim et al., 2002). No significant difference was observed between wild-type (n = 16, 4 mice) and mutant cells (n = 17, 4 mice) in the basal (+/+, 80.4 ± 3.23 nM; −/−, 80.9 ± 4.24 nM) or peak values (+/+, 330.67 ± 19.54 nM; −/−, 307.57 ± 30.19 nM) of $[Ca^{2+}]_i$ after stimulation by glutamate. However, the recovery of $[Ca^{2+}]_i$ to the basal level following the removal of glutamate was significantly slower in the mutant compared to wild-type cells (Figure 3C). The decay constant (τ), which was obtained by fitting a single exponential to the data, was about 40% larger in mutant (τ = 26.25 ± 6.21 s) than wild-type (τ = 9.96 ± 1.14 s) cells. These results indicate that NCX plays a role in restoring baseline Ca^{2+} levels following depolarization in the hippocampal pyramidal neurons, a finding consistent with results obtained in other cells (Ranciat-McComb et al., 2000; Tang et al., 2000; Domotor et al., 1999; Fierro et al., 1998; Sanchez-Armass and Blaustein, 1987).

Basal Synaptic Transmission in NCX2 Mutant Mice

To establish whether basal synaptic function is normal in NCX2 mutant mice, we recorded field excitatory postsynaptic potentials (fEPSPs) from area CA1 of the hippocampus in response to stimulation of Schaffer collateral fibers. As illustrated in Figures 4A–4C, the input-output

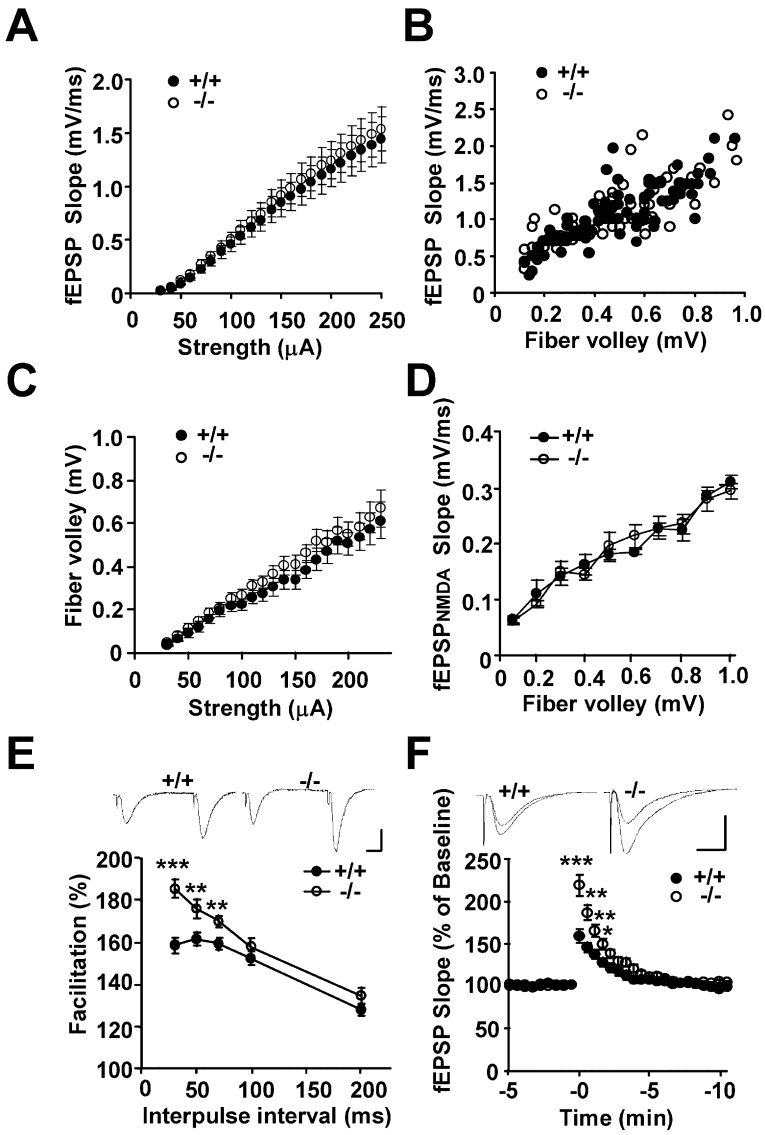

Figure 4. Normal Basal Synaptic Transmission but Enhanced STP in Mutants

(A) Input-output plot of synaptic transmission between stimulation strength and the corresponding fEPSP slope (wild-type, 13 slices, 4 mice; mutant, 13 slices, 5 mice).

(B) The slope of fEPSPs elicited by a given presynaptic fiber volley.

(C) Plot of synaptic transmission between stimulation strength and presynaptic fiber volley amplitude (wild-type, 15 slices, 5 mice; mutant, 14 slices, 5 mice).

(D) NMDA receptor-mediated synaptic potential in the presence of CNQX (10 μM) and reduced Mg^{2+} (0.1 mM) (wild-type, 7 slices, 3 mice; mutant, 8 slices, 3 mice).

(E) PPF is increased in mutant (wild-type, 19 slices, 8 mice; mutant, 20 slices, 7 mice). Traces are responses during PPF at 50 ms interval interpulse in wild-type (left) and mutant (right). $^{**}p < 0.01$, $^{***}p < 0.001$, Student's t test. Scale bars equal 1 mV and 10 ms.

(F) PTP performed with 50 μM D-AP5 (wild-type, 12 slices, 4 mice; mutant, 17 slices, 5 mice). $^{***}p < 0.001$, $^{**}p < 0.01$, $^{*}p < 0.05$, Student's t test. Scale bars equal 2 mV and 10 ms.

relation of synaptic transmission was not altered in mutant. We also measured the NMDA receptor-mediated component of fEPSPs by adding CNQX, an AMPA receptor blocker, to the buffer with reduced Mg^{2+} (Figure 4D). No significant difference was noted between the wild-type and the mutant in these NMDA receptor-mediated field responses. Together, these results indicate that the NCX2 mutation had no significant effect upon the basal synaptic function.

Enhanced Short-Term Plasticity in NCX2 Mutant Mice

Since Ca^{2+} is known to be involved in the regulation of synaptic transmission, we next studied the effect of the NCX2 mutation on two presynaptic forms of short-term plasticity (STP). First, we measured paired-pulse facilitation (PPF), a transient enhancement of neurotransmitter release induced by two closely spaced stimuli. This increase in release is usually attributed to residual Ca^{2+} in the presynaptic terminal following the first stimulus (Regehr et al., 1994). As expected from the delayed Ca^{2+} clearance in the NCX2 mutant neurons, PPF was significantly enhanced in the mutant compared to the wild-type at interpulse intervals below 100 ms (at interval of 30 ms, $p < 0.001$; 50 ms, $p < 0.01$; 70 ms, $p < 0.01$, Student's t test) (Figure 4E).

As a second measure of short-term plasticity, we examined posttetanic potentiation (PTP), a short-term form of presynaptic plasticity elicited by high-frequency tetanus. In the presence of D-AP5 to block NMDA receptors, a single 100 Hz tetanus stimulation resulted in an enhancement of EPSP that decayed to the baseline within 3 min. The mutant exhibited a higher peak of PTP than the wild-type (+/+, 157.1% ± 8.4% peak potentiation; −/−, 218.3% ± 11.3%, $p < 0.001$, Student's t test) (Figure 4F). Together, these data indicate that both forms of presynaptic short-term plasticity are enhanced in the NCX2 mutant mice.

Alteration of Long-Term Plasticity

We examined long-term potentiation (LTP) and long-term depression (LTD) using stimulation protocols in the

range 0.2–100 Hz. Administration of a single tetanus at 100 Hz elicited a significantly enhanced LTP in the mutant compared to that in the wild-type (−/−, 253.5% ± 8.2% of baseline at 50 min, n = 12; +/+, 143% ± 5.1%, n = 9, $p < 0.001$, Student's t test) (Figure 5A). With a 50 Hz tetanic stimulation, the mutant also exhibited a robust synaptic and nondecremental potentiation (−/−, 220.1% ± 25.1% of baseline at 50 min, n = 11; +/+, 124.3% ± 15.2%, n = 13, $p < 0.001$, Student's t test) (Figure 5B). Enhanced LTP in the mutant was also observed at 10 Hz stimulations, while only a marginal level of synaptic potentiation was induced in the wild-type (−/−, 158.2% ± 5.6% of baseline at 50 min, n = 12; +/+, 117.2% ± 6.0%, n = 10, $p < 0.001$, Student's t test) (Figure 5C).

Next, we tried to induce LTD in slices using low-frequency stimulation (LFS). As reported in the literature (Bear and Abraham, 1996), LFS did not elicit LTD in adult animals, so we studied LTD from 3- to 4-week-old mice. Stimulation at 1 Hz induced a depression of synaptic transmission within ~10 min in both wild-type and mutant. However, the depression was not maintained in the mutant slices unlike in the wild-type (−/−, 124.1% ± 6.6% of baseline at 50 min, n = 12; +/+, 81.5% ± 7.5%, n = 9, $p < 0.001$, Student's t test) (Figure 5D). Instead, potentiation was developed over time in the mutant slices. Basically similar results were obtained when the slices were stimulated at 0.5 Hz (−/−, 122.7% ± 9.8% of baseline at 50 min, n = 12; +/+, 72.5% ± 5.4%, n = 9, $p < 0.001$, Student's t test) (Figure 5E). However, stimulations at 0.2 Hz produced clear LTD in the mutant unlike in the wild-type (−/−, 76.7% ± 6.1% of baseline at 120 min, n = 7; +/+, 95.1% ± 4.5%, n = 6, $p < 0.01$, Student's t test) (Figure 5F).

As described above, $[Ca^{2+}]_i$ remains high for a prolonged time after stimulation in the neurons of the NCX2-deficient mice. The suppression of LTD at 1 Hz stimulation in the mutant slices could be due to the high level of $[Ca^{2+}]_i$ resulting from delayed kinetics of Ca^{2+} clearance. To examine whether the elevated level of $[Ca^{2+}]_i$ is responsible for this phenotype, we repeated the experiments using a stimulation protocol of 1 Hz in the presence of 2 μM D-AP5 to partially block the Ca^{2+} influx via NMDA receptors (Mizuno et al., 2001; Cummings et al., 1996). Under these conditions, LTD was induced in mutant slices (−/−, 85.2% ± 4.1% of baseline at 50 min, n = 8) as efficiently as in the wild-type (+/+, 81.5% ± 7.5% of baseline at 50 min, n = 9) (Figure 5D), indicating that the elevated level of Ca^{2+} due to delayed clearance can be responsible for the suppression of LTD generation in the NCX2 mutant.

In summary, the mutant slices exhibited a strong tendency for developing enhanced LTP. These results are summarized as a plot of plasticity versus stimulation frequency in Figure 5G. It is apparent that the frequency sensitivity of LTP and LTD induction in the CA1 region of the hippocampus is drastically shifted to lowered stimulus frequencies in NCX2 mutant mice.

Enhanced Spatial Learning and Memory in NCX2 Mutant Mice

We then examined whether the increased LTP in NCX2 mutant mice affected the animal's capacity for spatial learning and memory. First, we subjected the mice to the Morris water maze test (Morris et al., 1982). There was no difference in the swim speed between wild-type and mutant mice (Figure 6B). During acquisition, both wild-type (n = 12) and mutant (n = 13) mice exhibited a decreased escape latency during day sessions [$F(6,138) = 30.29$, $p < 0.0001$, two-way repeated ANOVA] (Figure 6A), indicating effective learning of the platform position. However, mutant mice displayed significantly shorter escape latencies than wild-type throughout day sessions, indicating that spatial learning was faster in mutant mice than in wild-type mice [$F(1,23) = 7.67$, $p < 0.01$, two-way repeated ANOVA]. Moreover, a post hoc test (Scheffe's test) revealed significant differences between the two genotypes at day 2 ($p < 0.05$), day 3 ($p < 0.05$), and day 5 ($p < 0.05$) sessions. In addition, enhanced spatial learning in mutant mice was also evident in the first probe test conducted after the third day session (Figures 6D and 6E). In this test, both wild-type and mutant mice spent more time in the target quadrant than in the other quadrants [$F(3,69) = 31.99$, $p < 0.0001$, two-way repeated ANOVA] and crossed platform sites more often than the alternate sites [$F(3,69) = 17.43$, $p < 0.0001$, two-way repeated ANOVA]. However, mutant mice spent more time in the target quadrant than wild-type mice (Student's t test, $p < 0.05$) (Figure 6D) and showed a more precise memory for the platform position, which is estimated by the number of platform crossings (Student's t test, $p < 0.05$) (Figure 6E). On the second probe test conducted after the seventh day sessions, both wild-type and mutant mice exhibited the same level of strong preference for the target quadrant (Figures 6F and 6G), indicating that the two groups eventually reached a same level of learning and memory.

We then carried out a visible platform test for three days to assess whether the enhanced learning and memory of the mutant mice was due to changes in the sensorimotor system or motivational or emotional status. There was no difference between the wild-type (n = 11) and mutant (n = 10) mice in the latency to escape (Figure 6C). From this, we could exclude the possibility that nonassociative factors might have affected the water maze performance of the tested animals.

Enhanced Contextual Fear Conditioning in NCX2 Mutant Mice

We next subjected the mice to the context-dependent fear conditioning assay, which is also known to require the function of the hippocampus (Phillips and LeDoux, 1992). The wild-type (n =12) and mutant (n = 12) mice showed similar levels of freezing response immediately after the training (Figure 7A). Mice were returned to the same shock chamber 24 hr after the training for fear memory. Both the wild-type and mutant mice displayed freezing, but the mutant mice displayed more freezing behavior than did the wild-type [$F(1,22) = 15.37$, $p < 0.001$, two-way repeated ANOVA], indicating an enhanced long-term memory of the mutant mice for contextual fear conditioning. A post hoc test (Scheffe's test) also revealed significant differences between the two genotypes during the first ($p < 0.001$), the second ($p < 0.01$), the third ($p < 0.05$), and the fifth ($p < 0.05$) minutes (Figure 7B). On the other hand, no difference was observed between the wild-type (n = 12) and mutant (n =

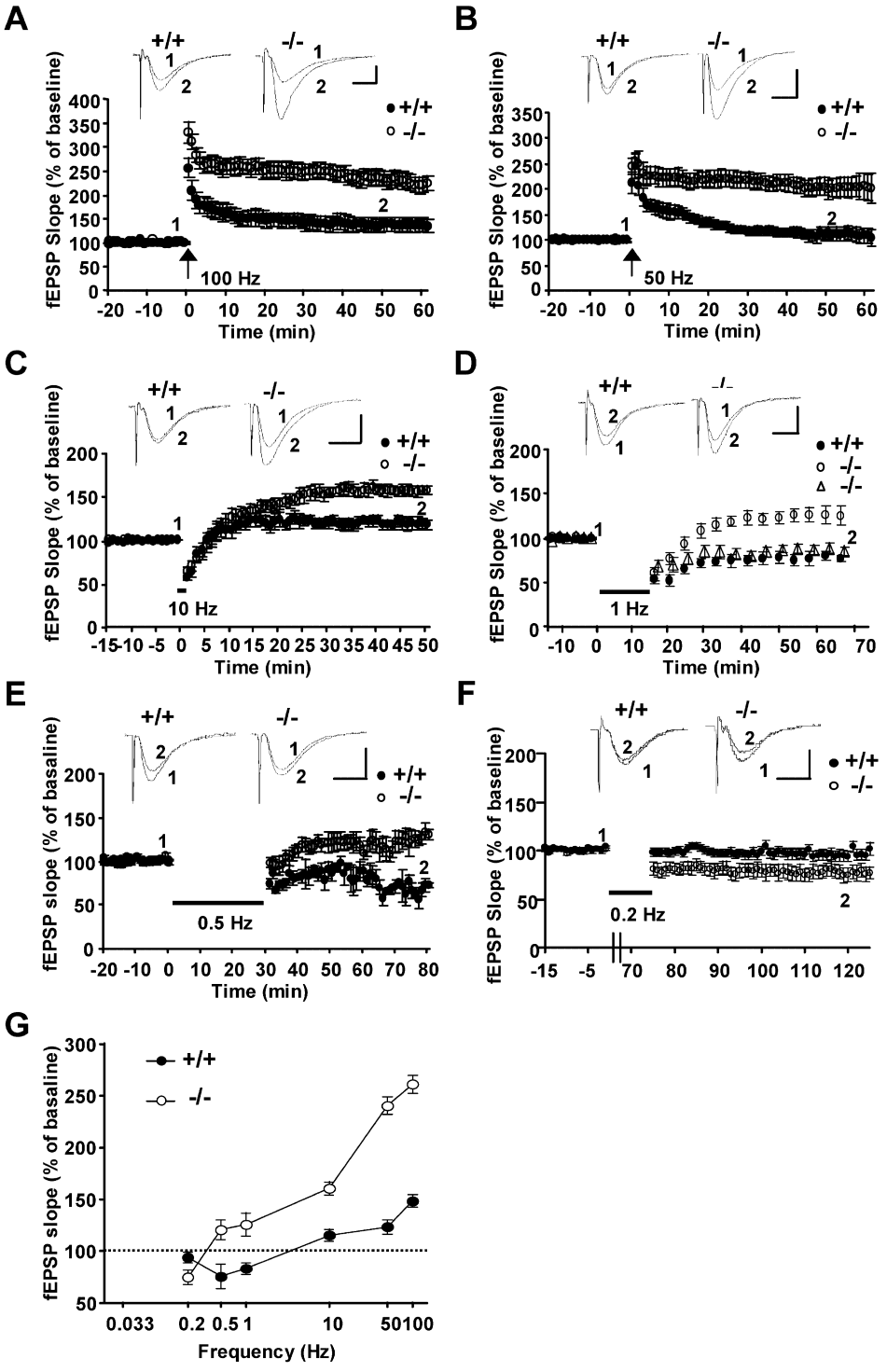

Figure 5. Long-Term Synaptic Plasticity

(A) LTP elicited by a single, 1 s 100 Hz train in mutant (12 slices, 10 mice) and wild-type (9 slices, 8 mice).

(B) LTP elicited by a single, 2 s 50 Hz train in mutant (11 slices, 5 mice) and wild-type (13 slices, 7 mice).

(C) LTP elicited by a single, 1.5 min 10 Hz train in mutant (12 slices, 7 mice) and wild-type (10 slices, 7 mice).

(D) LTD elicited by a single, 15 min 1 Hz train in mutant (12 slices, 10 mice) and wild-type (9 slices, 8 mice). LTD elicited in the presence of D-AP5 (2 μM) in mutant (8 slices, 5 mice) (open triangle). To ease visualization, the values were taken every 5 min.

(E) LTD elicited by a single, 30 min 0.5 Hz train in mutant (12 slices, 10 mice) and wild-type (9 slices, 8 mice).

(F) LTD elicited by a single, 75 min 0.2 Hz train in mutant (7 slices, 5 mice) and wild-type (6 slices, 5 mice).

(G) Summary of synaptic plasticity at different stimulation frequencies.

Scale bars equal 1.5 mV and 10 ms.

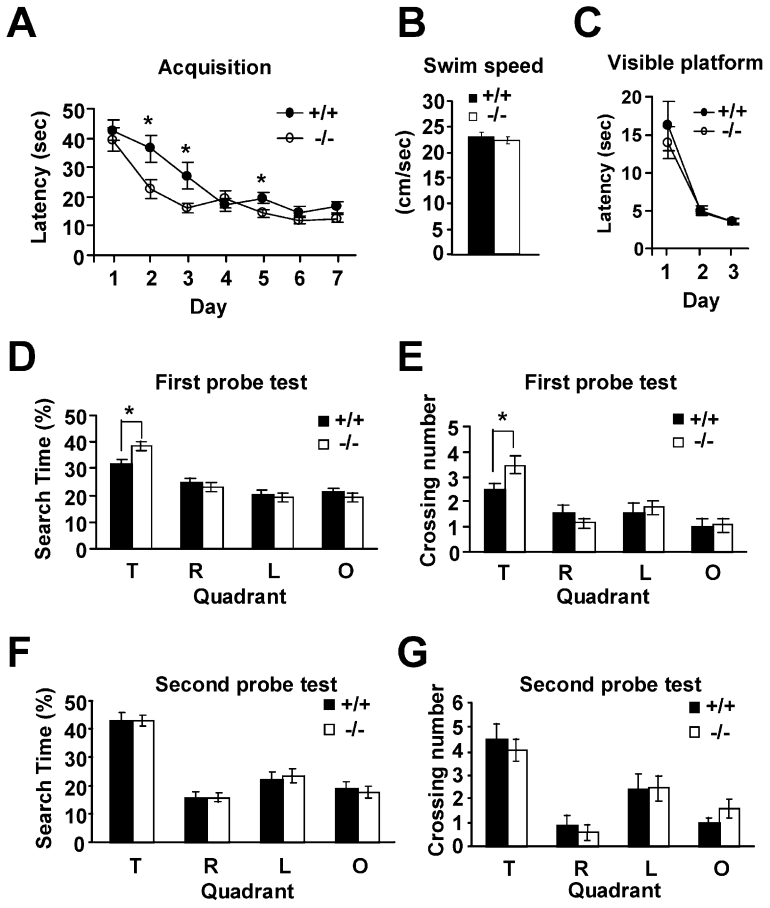

Figure 6. Enhanced Spatial Learning and Memory of NCX2 Mutant Mice in the Morris Water Maze.

(A) Mean escape latency per day cross days during 7 days training. Mutant mice (n = 13) have significantly lower escape latency during acquisition than wild-type mice (n = 12). *p < 0.05, Scheffe's post hoc test.

(B) Normal swim speed.

(C) A visible platform task over three training sessions (wild-type, 11 mice; mutant, 10 mice).

(D and E) The first probe test after day 3 training: Mutant mice spent more time in the target quadrant (D) and showed a more precise memory in crossing number for the target platform position (E). *p < 0.05, Student's t test.

(F and G) The second probe test after day 3 training.

Abbreviations: T, target quadrant; R, adjacent right quadrant; L, adjacent left quadrant; O, opposite quadrant).

12) mice in the cued fear conditioning assay (Figure 7C), indicating that the enhanced memory in NCX2 mutant mice is limited to hippocampus-dependent fear conditioning.

Enhanced Object Recognition Memory in NCX2 Mutant Mice

Lastly, we carried out novel object recognition task that is based on the discrimination between a familiar and

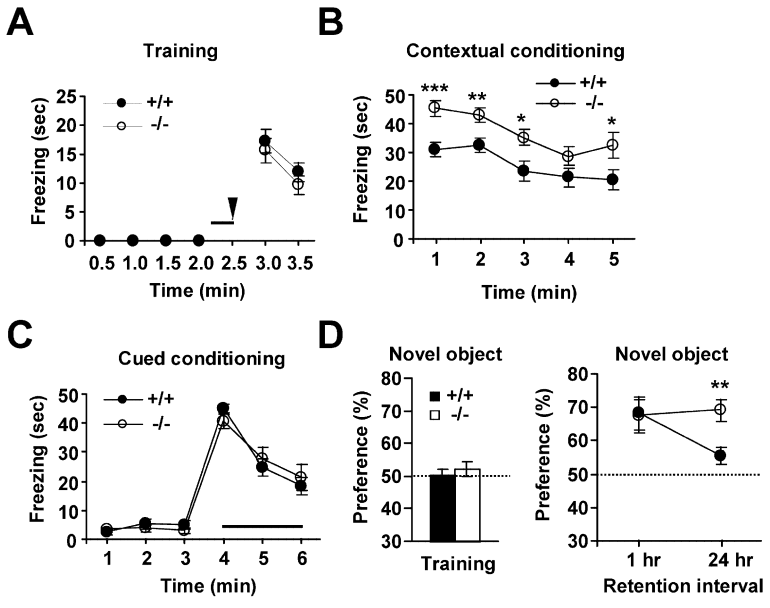

Figure 7. Enhancement of Context-Dependent Fear Conditioning and Novel Object Recognition Memory in NCX2 Mutant Mice

(A) Freezing behavior on the day of training in wild-type (n = 12) and mutant (n = 12). Solid line indicates the duration of CS (tone, 20 s) and the triangle indicates US (foot shock, 2 s).

(B) Contextual fear conditioning 24 hr after training. ***p < 0.001, **p < 0.01, *p < 0.05, Scheffe's post hoc test.

(C) Cued fear conditioning 24 hr after training. CS (tone) presentation is indicated by the solid line.

(D) Novel object recognition task. Mean exploratory preference during training in wild-type (n = 15) and mutant mice (n = 16) (left). Exploration to a novel object during each retention time (right). **p < 0.01, Scheffe's post hoc test.

Dotted line indicates equal exploration of all objects.

a novel object, which requires the hippocampus (Vnek and Rothblat, 1996). We first assessed the amount of time spent exploring the two objects during the training trial, and there was no difference between wild-type ($n = 15$) and mutant mice ($n = 16$) (Figure 7D, left), which indicates no preference for either object. At 1 hr retention interval, both wild-type ($n = 6$) and mutant mice ($n = 7$) exhibited increased preference for the novel object than to the familiar one [$F(1,11) = 14.55$, $p < 0.01$, two-way repeated ANOVA], but no difference was found between wild-type and mutant mice [$F(1,11) = 0.01$, $p = 0.96$]. At 24 hr retention, however, mutant mice ($n = 9$) showed increased preference for the novel object compared to wild-type ($n = 9$) [$F(1,16) = 16.48$, $p < 0.001$, two-way repeated ANOVA, Scheffe's post hoc test, $p < 0.01$] (Figure 7D, right), indicating that the mutant mice have an enhanced performance in the object recognition memory task.

Discussion

The main conclusion of the present study is that the deletion of NCX2 function in hippocampal neurons prolongs the time required for clearance of the increased $[Ca^{2+}]_i$ induced by neuronal activation and biases synaptic plasticity toward increased STP and LTP, thereby enhancing the animal's capacity for learning and memory that requires the function of the hippocampus. These studies demonstrate that NCX2-mediated Ca^{2+} homeostasis is critical for the control of synaptic plasticity and cognition.

Short-Term Synaptic Plasticity in NCX2 Mutant Mice

Presynaptic $[Ca^{2+}]_i$ measurements and manipulation of presynaptic exogenous buffers revealed roles for residual $[Ca^{2+}]_i$ following conditioning stimulation in short-term synaptic enhancement (Regehr et al., 1994; Zucker, 1999). NCX not only plays a role in reducing $[Ca^{2+}]_i$ in individual presynaptic terminals after electrical stimulation, but is also involved in the regulation of exocytosis of synaptic vesicles (Reuter and Porzig, 1995). Blockade of Ca^{2+} efflux via NCX enhances neurotransmitter release from brain synaptosomes (Sanchez-Armass and Blaustein, 1987) and hippocampal neurons (Bouron and Reuter, 1996). The present observation of enhanced PPF in the hippocampal slices of NCX2 mutant mice indicates that NCX2 is the major isoform involved in the clearance of Ca^{2+} in presynaptic terminals.

Increase in $[Ca^{2+}]_i$ is essential for the generation of PTP (Delaney and Tank, 1994), and a large Na^+-induced increase of $[Ca^{2+}]_i$ is sufficient to enhance transmitter release and to increase PTP (Wojtowicz and Atwood, 1985). NCX currents are considered important in the regulation of PTP in synapses, since the accumulation of Na^+ in nerve terminals during and after tetanic stimulation causes an increase in $[Ca^{2+}]_i$ by reducing the driving force for extrusion of Ca^{2+} by NCX or by reversing the direction of NCX (Mulkey and Zucker, 1992). These results indicate that a dynamic regulation of $[Ca^{2+}]_i$ in the presynaptic sites by NCX is crucial for proper control of the number of transmitter quanta in the hippocampal neurons and that the NCX2 plays an important role in this process.

NCX2 as a Temporal Factor in the Regulation of Long-Term Synaptic Plasticity

The role of a postsynaptic rise of $[Ca^{2+}]_i$ in the induction of LTP and LTD has been well established (Lynch et al., 1983; Mulkey and Malenka, 1992; Zucker, 1999). There are many reports showing the importance of both the levels and the duration of elevated $[Ca^{2+}]_i$ in synaptic plasticity. Recent reports (Yang et al., 1999; Cho et al., 2001) showed that LTP and LTD could be selectively induced according to intracellular Ca^{2+} concentration. Although the specificity of Ca^{2+} signaling can be achieved not only by amplitude but also by the frequency and duration of the calcium transient (Dolmetsch et al., 1997; Berridge, 1997), the effects of changing amplitudes of Ca^{2+} transients on synaptic plasticity have been extensively documented, but not so the effects of temporal changes. Our paper addresses this issue and the results suggest that NCX2 can be a critical temporal factor in the regulation of the postsynaptic $[Ca^{2+}]_i$ and thus determine the sign of synaptic modification. In the NCX2 mutant, LFS may cause higher Ca^{2+} levels compared to wild-type when calcium clearance is delayed by the deficiency of NCX2, thereby enhancing LTP at the expense of LTD. Consistent with this idea, a partial blockade of NMDA receptors, which limits the Ca^{2+} influx, promoted LTD in the mutant. Not only the amplitude but also the duration of elevated Ca^{2+} could be critical determinants in the differential induction of LTP or LTD (Mizuno et al., 2001). One of the physiological mechanisms for regulating the balance for LTP versus LTD could be by controlling the duration of the increased postsynaptic Ca^{2+} signal through modulation of the NCX2 function.

It was shown that a brief and high Ca^{2+} elevation induced by HFS triggered LTP through activation of a CaMKII- and PKA-dependent process, whereas a prolonged and moderate Ca^{2+} elevation induced by LFS triggered LTD through activation of a phosphatase, calcineurin-PP1 cascade (Lisman, 1989; Lisman and Zhabotinsky, 2001; Soderling and Derkach, 2000; Lisman et al., 2002). After and during the HFS and LFS in the NCX2 mutant, Ca^{2+}-mediated activities or modifications of these kinases/phosphatases and their various substrates (e.g., AMPA and NMDA receptor) might be changed to favor LTP. It is interesting to compare our NCX2 results with those of others concerned with Ca^{2+} signaling and long-term synaptic plasticity. Transgenic mice expressing a constitutively active calcium-independent Ca^{2+}/calmodulin-dependent protein kinase II (CaMKII-T286D) exhibited an enhanced 5 Hz LTP at low levels of this transgene expression (Bejar et al., 2002). This result suggests that the primary effect of a constitutively active CaMKII is to facilitate LTP. In this aspect, this transgenic mouse is similar to our $NCX2^{-/-}$ mice. However, 5 Hz LTP was impaired at high levels of transgene expression, which is similar to their initial result (Mayford et al., 1995), as would be predicted by the ability of active CaMKII to occlude LTP (Lledo et al., 1995). However, compared to $NCX2^{-/-}$ mice that showed an improvement in spatial and nonspatial learn-

ing tasks, CaMKII-T286D mice exhibited impaired ability in learning and memory even in the visible platform task. This behavioral difference could have resulted from a compensatory change in the expression of genes associated with inhibitory neurotransmission that may have occurred in the CaMKII-T286D mice (Bejar et al., 2002). On the other hand, CaMKII-T286A mutant mice that were unable to switch CaMKII to its CaM-independent state showed lower LTP levels at several stimulation frequencies and exhibited learning impairments (Giese et al., 1998), a mirror-image phenotype to that of NCX2 mutant mice.

From our results, we propose a model as to how NCX2 contributes to the cellular state determining whether synapses are to be potentiated or depressed. In this model we propose a term, "strength of Ca^{2+} signal," which is determined by both the magnitude and the duration of the increased $[Ca^{2+}]_i$. NCX2 functions as a negative temporal regulator for the increased $[Ca^{2+}]_i$ by facilitating Ca^{2+} clearance. An enhanced NCX2 activity will lead to a decrease in the strength of the Ca^{2+} signal, whereas a suppressed NCX2 activity will result in the opposite effect, an increase of the Ca^{2+} signal strength. The activities of Ca^{2+}-dependent molecules related to synaptic weight will be differentially regulated depending on the strength of this signal: a "stronger" signal will activate a CaMKII- and PKA-dependent process leading to LTP, whereas a "weaker" signal will trigger LTD through activation of a phosphatase, calcineurin-PP1 cascade. NCX2 could thus act as a cellular switch to determine the direction of synaptic plasticity. In this regard it is interesting to note that NO and cGMP can reduce NCX activity with increasing presynaptic $[Ca^{2+}]_i$ (Meffert et al., 1994; Asano et al., 1995). Since such regulatory effects may act at both pre- and postsynaptic sites, it is possible that activity-dependent NCX regulation could be used to set temporal constraints on the strength of the calcium signal and thus the potential for synaptic plasticity.

LTP and Hippocampus-Dependent Learning and Memory in Genetically Engineered Mice

Activity-dependent synaptic plasticity is thought to be the cellular mechanism for storing new information in the brain. Previous studies indicated that activity-dependent increases in postsynaptic $[Ca^{2+}]_i$ and subsequent activation of Ca^{2+}-dependent enzymes play a critical role in synaptic plasticity that may serve as a cellular cognate of memory acquisition and consolidation (Bliss and Collingridge, 1993; McGaugh, 2000). Our results are consistent with this paradigm. Improved cognitive performance of NCX2 mutant mice was observed in three different hippocampus-dependent tasks (water maze, context fear conditioning, and object recognition memory). Both the formation of a new memory and the long-term storage of the memory were improved.

There are several reports of genetically engineered mice related to activation and balance of kinases (such as CaMKII and PKA) and phosphatases (such as calcineurin and PP1) after Ca^{2+} influx through NMDA receptors, which exhibit enhanced or impaired LTP and learning. A mouse in which the deletion of the NMDAR1 gene is restricted to the CA1 hippocampus lacked LTP and exhibited impaired spatial memory (Tsien et al., 1996). Tang et al. (1999) showed that overexpression of NMDA receptor 2B (NR2B) enhanced LTP and both spatial and nonspatial learning in the mouse. NR2B expression is normally downregulated in adults, while NCX2 expression is upregulated in adults. Although the enhanced LTP in NCX2 mutant mice was NMDA receptor dependent, the enhanced learning and memory does not appear to be due to changes in NMDA receptor itself, since NMDA receptor-mediated fEPSPs were unaltered in the mutant.

There have been many reports of transgenic mice having altered or modified CaMKII following the initial reports by Silva et al. (1992a, 1992b), and their results demonstrated that CaMKII is required for LTP and spatial learning (Lisman et al., 2002). Together with CaMKII results, work on the calcineurin-PP1 cascade provides some insight into the signaling mechanism of LTP and learning. Overexpression of calcineurin in mice depressed LTP and impeded the formation of long-term memory (Mansuy et al., 1998; Winder et al., 1998). These results led to an effort to genetically engineer mice in an attempt to enhance LTP and memory. Malleret et al. (2001) reported that LTP and learning and memory were reversibly enhanced in various hippocampus-dependent learning tasks in mutant mice with a transiently reduced calcineurin activity obtained by the dominant-negative approach. Furthermore, mice expressing a constitutively active form of the PP1 inhibitor exhibited a reduced PP1 activity and showed improved performance in water maze and object recognition tasks (Genoux et al., 2002). It will be interesting to examine if this cascade is under the control of NCX2 functions.

In this study, we attempted to define the role of NCX2 in the brain using mice lacking NCX2. Our results demonstrate that mutant mice exhibit an improvement in learning and memory capacity together with enhanced LTP. The data support the hypothesis that LTP correlates with learning and memory (Martin et al., 2000). NCX2 may be a possible target for future drug development directed toward improving the cognitive function of patients suffering from a cognitive impairment, such as Alzheimer's disease (Colvin et al., 1991).

Experimental Procedures

Generation of NCX2 Knockout Mice

Murine *NCX2* gene sequences were isolated from a mouse strain 129/Sv genomic phage library (lambda FIX II, Stratagene) using a rat cDNA probe (Li et al., 1994). The exon 1 was in-frame replaced at start codon (ATG) with 1.7 kb of NLS-Cre from pxCANCre (NLS, nuclear localization sequence; Cre, cre recombinase) (Kanegae et al., 1995). The targeted ES clones were identified by Southern blot analysis and used in the generation of germline chimeras, as previously described (Kim et al., 1997). Male chimeras were crossed with female C57BL/6J mice to derive germline-transmitted F1 heterozygotes ($NCX2^{+/-}$), and these F1 heterozygotes were intercrossed to derive homozygous mutant mice ($NCX2^{-/-}$).

The mice used for analysis had F2 genetic backgrounds of 129/Sv and C57BL/6J. Animal care and handling were carried out according to institutional guidelines. The mice were maintained with free access to food and water under a 12:12 hr light:dark cycle with the light cycle beginning at 6:00 a.m. Mice aged 8–12 weeks were used in behavior tasks. Some of the physiological experiments were performed at young age (2–3 weeks old) due to technical limitations. But this should not cause a major concern, since the level of tran-

scripts of NCX2 peaks after PND 14 and maintained thereafter (Sakaue et al., 2000; Gibney et al., 2002).

RT-PCR

Total RNA was isolated from brain and skeletal muscle (the upper thigh of the hindlimbs) of pup and adult wild-type mice using TRIzol® Reagent and amplified according to the manufacturer's protocol (GIBCO-BRL). cDNA was amplified by PCR with DyNAzyme™II DNA polymerase (Finnzymes Inc.). The 5′ primer was 5′-ATGGCTCCCTT GGCTTTGATG-3′ and 3′ primer was 5′-ACCCAGGAACATGTAGAC CATG-3′. RT-PCR products were separated on a 2% agarose gel.

Northern Blot and Western Blot Analyses

Total RNA (20 μg) was isolated from brains by homogenization with TRIzol® Reagent (GIBCO), electrophoresed on a 1% agarose gel containing formaldehyde, and transferred onto nylon membranes with 10× SSC for 20 hr. After UV crosslinking, the membranes were hybridized for 20 hr at 65°C to [α-^{32}P]dCTP-labeled 1060 bp *Pac* I/*Not* I-digested fragment from pxCANCre. The membrane was washed for 10 min at room temperature in 2× SSC and 1% SDS. After two further washes for 15 min at 65°C in 0.2× SSC and 1% SDS, the membrane was exposed to autoradiography.

For Western blotting, whole brains were isolated from mice, homogenized, and sonicated in a cold lysis buffer (20 mM HEPES, 150 mM NaCl, 1% Triton X-100, 1 mM PMSF, complete protease inhibitor cocktail [Boehringer Mannheim], Calpain inhibitors I and II). After low-speed centrifugation (1000 × g for 5 min at 4°C), supernatants were centrifuged (28,000 × g for 15 min at 4°C) to obtain crude membrane fractions. The crude membrane fractions were separated in SDS-PAGE gels (8%), blotted to nitrocellulose membranes, and visualized with the primary antibody (anti-NCX2, 1:10,000 dilution) by enhanced chemiluminescence (ECL), as previously described (Kim et al., 2001).

Histology

For cresyl violet staining, mice were transcardially perfused with 4% paraformaldehyde in 0.1 M phosphate buffer (pH 7.4) and fixed at 4°C. After embedding in paraffin wax according to the standard procedure, sections of 8 μm were prepared using a microtome. Tissue sections were deparaffinized, washed, incubated with 90% alcohol at 37°C for 12 hr, and then stained with cresyl violet for 2 hr.

For X-gal staining, brains (NCX 2$^{+/-}$-CAG-CAT-Z) were fixed, sectioned (50–70 μm), washed three times with phosphate-buffered saline, and incubated in LacZ staining solution (0.05 M phosphate buffer, 5 mM $K_3Fe(CN)_6$, 5 mM $K_4Fe(CN)_6$, 2 mM $MgCl_2$, 1 mg/ml X-gal) at 30°C overnight (Sakai and Miyazaki, 1997).

Whole-Cell Patch-Clamp Analysis

Whole-cell voltage-clamp recording was performed according to modifications of methods described by Fierro et al. (1998). All experiments were carried out using hippocampal slices of 250 μm thickness prepared from 2- to 3-week-old mice. Cells were voltage-clamped at −40 mV using whole-cell electrodes (3–5 MΩ, series resistance <20 MΩ). Pipettes were filled with solution containing 3 mM NaCl, 114 mM CsCl, 9 mM EGTA, 9 mM HEPES, 1.8 mM $MgCl_2$, 4 mM MgATP, 0.3 mM Tris-GTP, 5.4 mM $CaCl_2$, H_2CaEGTA (added to obtain an estimated free Ca^{2+} concentration of 100 nM at room temperature) with the pH adjusted to 7.4 with CsOH. Contaminating currents arising from the activation of the Na^+/K^+ pump and K^+-dependent NCX (NCKX) (Tsoi et al., 1998) were blocked by using TEA-Cl in the K^+-free external buffer. Experiments were performed at room temperature with the use of an EPC-9 amplifier and Pulse/Pulsefit software (HEKA, Germany). All data were expressed as the mean ± SEM. All experiments were performed in the presence of 5 mM tetraethylammonium chloride (TEA), 1 μM tetrodotoxin (TTX), and 10 μM bicucullin. Student's t test was used for statistical analyses.

Intracellular Ca^{2+} Measurement in Hippocampal CA1 Neurons

Hippocampal slices (400 μm) were obtained from 2- to 3-week-old mice as described in Extracellular Recording (see below). Hippocampal slices were kept for 1 hr in ACSF and treated enzymatically with Neurobasal-A medium (GIBCO-BRL, Grand Island, NY) containing 0.1% papain (Roche) for 30 min at 32°C. CA1 pyramidal regions were then dissected out, triturated about five times with a fire-polished Pasteur pipette, and plated onto poly-L-lysine-coated coverslips. The intracellular Ca^{2+} was measured using fura-2 acetoxymethyl ester (fura-2/AM) as a Ca^{2+} indicator in cell bodies, as previously described (Kim et al., 2002). Following the incubation period (60 min), neurons were washed three times with buffer and exposed to 250 μM glutamate for 10 s, and the decline in $[Ca^{2+}]_i$ was monitored over the next 4–5 min. This was repeated three times for each set of neurons.

Extracellular Recording in Hippocampal CA1

Hippocampal slices (400 μm) from 7- to 8-week-old mice were prepared in oxygenated cold ACSF (124 mM NaCl, 3.5 mM KCl, 1.25 mM NaH_2PO_4, 2 mM $CaCl_2$, 1.3 mM $MgSO_4$, 26 mM $NaHCO_3$, and 10 mM glucose at pH 7.4). Slices were then placed at an interface of air and ACSF in a warm, humidified (32°C, 95% O_2/5% CO_2) recording chamber and maintained for 1.5 hr prior to the experiments. A bipolar stimulating electrode was placed in the stratum radiatum in the CA1 region, and extracellular field potentials were also recorded in the stratum radiatum using a glass microelectrode (borosilicate glass, 3–5 MΩ, filled with 3 M NaCl), as previously described (Jun et al., 1998). Test responses were elicited at 0.033 Hz. For LTP experiments, baseline stimulation was delivered at an intensity that evoked a response approximately 40% of the maximum evoked response. Mice used for LTD were 3–4 weeks old. Drugs were added to the perfusion medium at least 30 min before recording. Data are given as mean ± SEM. Student's t test was used for statistical analyses.

Morris Water Maze

The water maze apparatus consisted of a circular pool (white plastic, 120 cm diameter, 93 cm height) containing water at 24°C–26°C. The water was rendered opaque white by adding nontoxic water-soluble paint. The pool was located in the center of a room (2.5 × 2.5 min) in which four different distal cues were hung on the four walls high enough to be seen from the pool, as previously described (Jun et al., 1998). The animals were trained to find the hidden platform for seven sessions (four trials per session per day). Two probe tests were performed after the third day of training and the seventh day of training. In the visible platform task, different animals were placed in the same water maze used in the hidden platform task with two differences in the procedure: (1) there were three trials per session per day, and (2) the platform was colored black and moved in every trial.

Fear Conditioning

A fear-conditioning shock chamber (19 × 20 × 33 cm) containing a stainless steel rod floor (5 mm diameter, spaced 1 cm apart) and a monitor was used (WinLinc Behavioral Experimental control software, Coulbourn Instruments). For conditioning (Lu et al., 1997), mice were placed in the fear-conditioning apparatus chamber for 2 min, and then a 20 s acoustic conditioned stimulus (CS) was delivered. During the last 2 s of the tone, a 0.5 mA shock of unconditioned stimulus (US) was applied to the floor grid. This protocol was performed once. In order to assess contextual learning, the animals were placed back into the training context 24 hr after training and observed for freezing for 5 min. In order to assess cued learning, the animals were placed in a different context (novel chamber, odor, floor, and visual cues) 24 hr after training, and their behaviors were monitored for 6 min. During the last 3 min of this test, animals were exposed to the tone. Fear response was quantified by measuring the length of the time when the animal showed freezing behaviors with a stopwatch. Freezing behavior was defined as lack of movements with a crouching position, except for respiratory movements. In addition to freezing response, animals' locomotor activity was recorded by an infrared activity monitor built in the apparatus.

Novel Object Recognition Memory Task

The task was performed as described (Mansuy et al., 1998; Tang et al., 1999; Podhorna and Brown, 2002). Thirty-one animals (+/+, 1 hr, n = 6; +/+, 24 hr, n = 9; −/−, 1 hr, n = 7; −/−, 24 hr, n = 9) were individually habituated to an open-field box (40 × 40 × 40 cm)

for 3 days. During the training trial, two objects were placed in the box and animals were allowed to explore them for 5 min. A mouse was considered to be exploring the object when its head was facing the object within 1 inch. Following retention intervals (1 hr or 24 hr), animals were placed back to the box with two objects in the same locations, but one of the familiar objects was replaced by a novel object and then were allowed to explore the two objects for 5 min. The preference percentage, ratios of the amount of time spent exploring any one of two objects or the novel one over the total time spent exploring both objects, were used to assess the recognition memory.

Data Analyses in Behavior

Statistical analyses were conducted using SAS. Two-way repeated ANOVA was used for behavioral analyses with genotype as the between subject factor, and time (object recognition), day, quadrant, platform crossings (Morris water maze), or time (fear conditioning) as within subject factors. A post hoc test and Student's t test were used to see which contributes to the main effect. Data are given as mean ± SEM.

Acknowledgments

The authors thank J. Myazaki for providing us with the CAG-CAT-Z and CAG-Cre mice, S.C. Lee and O.K. Lee for help in slice recording, S. Kim for help in Ca^{2+} imaging, M.P. Kong for help in ES cell injection, C. Kim for help in ES cell culture, Y. Namkung, Y. Choi, and J. Park for help in behavior experiments, and D.P. Wolfer and A. Kirkwood for critical comments on the manuscript. This work was supported by the National Creative Research Initiative Program, Ministry of Science and Technology, Korea, and Chemoinformatics Project of Korea Institute of Science and Technology.

Received: July 23, 2002
Revised: April 28, 2003
Accepted: May 23, 2003
Published: June 18, 2003

References

Asano, S., Matsuda, T., Takuma, K., Kim, H.S., Sato, T., Nishikawa, T., and Baba, A. (1995). Nitroprusside and cyclic GMP stimulate Na^+-Ca^{2+} exchange activity in neuronal preparations and cultured rat astrocytes. J. Neurochem. *64*, 2437–2441.

Bear, M.F., and Abraham, W.C. (1996). Long-term depression in hippocampus. Annu. Rev. Neurosci. *19*, 437–462.

Bejar, R., Yasuda, R., Krugers, H., Hood, K., and Mayford, M. (2002). Transgenic calmodulin-dependent protein kinase II activation: dose-dependent effects on synaptic plasticity, learning, and memory. J. Neurosci. *22*, 5719–5726.

Berridge, M.J. (1997). The AM and FM of calcium signalling. Nature *386*, 759–760.

Blaustein, M.P., and Lederer, W.J. (1999). Sodium/calcium exchange: its physiological implications. Physiol. Rev. *79*, 763–854.

Bliss, T.V., and Collingridge, G.L. (1993). A synaptic model of memory: long-term potentiation in the hippocampus. Nature *361*, 31–39.

Bouron, A., and Reuter, H. (1996). A role of intracellular Na^+ in the regulation of synaptic transmission and turnover of the vesicular pool in cultured hippocampal cells. Neuron *17*, 969–978.

Cho, K., Aggleton, J.P., Brown, M.W., and Bashir, Z.I. (2001). An experimental test of the role of postsynaptic calcium levels in determining synaptic strength using perirhinal cortex of rat. J. Physiol. *532*, 459–466.

Colvin, R.A., Bennett, J.W., Colvin, S.L., Allen, R.A., Martinez, J., and Miner, G.D. (1991). Na^+/Ca^{2+} exchange activity is increased in Alzheimer's disease brain tissues. Brain Res. *543*, 139–147.

Cummings, J.A., Mulkey, R.M., Nicoll, R.A., and Malenka, R.C. (1996). Ca^{2+} signaling requirements for long-term depression in the hippocampus. Neuron *16*, 825–833.

Delaney, K.R., and Tank, D.W. (1994). A quantitative measurement of the dependence of short-term synaptic enhancement on presynaptic residual calcium. J. Neurosci. *14*, 5885–5902.

Dolmetsch, R.E., Lewis, R.S., Goodnow, C.C., and Healy, J.I. (1997). Differential activation of transcription factors induced by Ca^{2+} response amplitude and duration. Nature *386*, 855–858.

Domotor, E., Abbott, N.J., and Adam-Vizi, V. (1999). Na^+-Ca^{2+} exchange and its implications for calcium homeostasis in primary cultured rat brain microvascular endothelial cells. J. Physiol. *515*, 147–155.

Fierro, L., DiPolo, R., and Llano, I. (1998). Intracellular calcium clearance in Purkinje cell somata from rat cerebellar slices. J. Physiol. *510*, 499–512.

Genoux, D., Haditsch, U., Knobloch, M., Michalon, A., Storm, D., and Mansuy, I.M. (2002). Protein phosphatase 1 is a molecular constraint on learning and memory. Nature *418*, 970–975.

Gibney, G.T., Zhang, J.H., Douglas, R.M., Haddad, G.G., and Xia, Y. (2002). Na^+/Ca^{2+} exchanger expression in the developing rat cortex. Neuroscience *112*, 65–73.

Giese, K.P., Fedorov, N.B., Filipkowski, R.K., and Silva, A.J. (1998). Autophosphorylation at Thr286 of the α calcium-calmodulin kinase II in LTP and learning. Science *279*, 870–873.

Hryshko, L.V., and Philipson, K.D. (1997). Sodium-calcium exchange: recent advances. Basic Res. Cardiol. *92*, 45–51.

Jun, K., Choi, G., Yang, S.G., Choi, K.Y., Kim, H., Chan, G.C., Storm, D.R., Albert, C., Mayr, G.W., Lee, C.J., and Shin, H.S. (1998). Enhanced hippocampal CA1 LTP but normal spatial learning in inositol 1,4,5-trisphosphate 3-kinase(A)-deficient mice. Learn. Mem. *5*, 317–330.

Kanegae, Y., Lee, G., Sato, Y., Tanaka, M., Nakai, M., Sakaki, T., Sugano, S., and Saito, I. (1995). Efficient gene activation in mammalian cells by using recombinant adenovirus expressing site-specific Cre recombinase. Nucleic Acids Res. *23*, 3816–3821.

Kim, D., Jun, K.S., Lee, S.B., Kang, N.G., Min, D.S., Kim, Y.H., Ryu, S.H., Suh, P.G., and Shin, H.S. (1997). Phospholipase C isozymes selectively couple to specific neurotransmitter receptors. Nature *389*, 290–293.

Kim, D., Song, I., Keum, S., Lee, T., Jeong, M.J., Kim, S.S., McEnery, M.W., and Shin, H.S. (2001). Lack of the burst firing of thalamocortical relay neurons and resistance to absence seizures in mice lacking α_{1G} T-type Ca^{2+} channels. Neuron *31*, 35–45.

Kim, S., Ahn, K., Oh, T.H., Nah, S.Y., and Rhim, H. (2002). Inhibitory effect of ginsenosides on NMDA receptor-mediated signals in rat hippocampal neurons. Biochem. Biophys. Res. Commun. *296*, 247–254.

Li, Z., Matsuoka, S., Hryshko, L.V., Nicoll, D.A., Bersohn, M.M., Burke, E.P., Lifton, R.P., and Philipson, K.D. (1994). Cloning of the NCX2 isoform of the plasma membrane Na^+-Ca^{2+} exchanger. J. Biol. Chem. *269*, 17434–17439.

Linck, B., Qiu, Z., He, Z., Tong, Q., Hilgemann, D.W., and Philipson, K.D. (1998). Functional comparison of the three isoforms of the Na^+/Ca^{2+} exchanger (NCX1, NCX2, NCX3). Am. J. Physiol. *274*, C415–423.

Lisman, J. (1989). A mechanism for the Hebb and the anti-Hebb processes underlying learning and memory. Proc. Natl. Acad. Sci. USA *86*, 9574–9578.

Lisman, J.E., and Zhabotinsky, A.M. (2001). A model of synaptic memory: a CaMKII/PP1 switch that potentiates transmission by organizing an AMPA receptor anchoring assembly. Neuron *31*, 191–201.

Lisman, J., Schulman, H., and Cline, H. (2002). The molecular basis of CaMKII function in synaptic and behavioural memory. Nat. Rev. Neurosci. *3*, 175–190.

Lledo, P.M., Hjelmstad, G.O., Mukherji, S., Soderling, T.R., Malenka, R.C., and Nicoll, R.A. (1995). Calcium/calmodulin-dependent kinase II and long-term potentiation enhance synaptic transmission by the same mechanism. Proc. Natl. Acad. Sci. USA *92*, 11175–11179.

Lu, Y.M., Jia, Z., Janus, C., Henderson, J.T., Gerlai, R., Wojtowicz, J.M., and Roder, J.C. (1997). Mice lacking metabotropic glutamate

receptor 5 show impaired learning and reduced CA1 long-term potentiation (LTP) but normal CA3 LTP. J. Neurosci. *17*, 5196–5205.

Lynch, G., Larson, J., Kelso, S., Barrionuevo, G., and Schottler, F. (1983). Intracellular injections of EGTA block induction of hippocampal long-term potentiation. Nature *305*, 719–721.

Malleret, G., Haditsch, U., Genoux, D., Jones, M.W., Bliss, T.V., Vanhoose, A.M., Weitlauf, C., Kandel, E.R., Winder, D.G., and Mansuy, I.M. (2001). Inducible and reversible enhancement of learning, memory, and long-term potentiation by genetic inhibition of calcineurin. Cell *104*, 675–686.

Mansuy, I.M., Mayford, M., Jacob, B., Kandel, E.R., and Bach, M.E. (1998). Restricted and regulated overexpression reveals calcineurin as a key component in the transition from short-term to long-term memory. Cell *92*, 39–49.

Martin, S.J., Grimwood, P.D., and Morris, R.G. (2000). Synaptic plasticity and memory: an evaluation of the hypothesis. Annu. Rev. Neurosci. *23*, 649–711.

Mayford, M., Wang, J., Kandel, E.R., and O'Dell, T.J. (1995). CaMKII regulates the frequency-response function of hippocampal synapses for the production of both LTD and LTP. Cell *81*, 891–904.

McGaugh, J.L. (2000). Memory—a century of consolidation. Science *287*, 248–251.

Meffert, M.K., Premack, B.A., and Schulman, H. (1994). Nitric oxide stimulates Ca(2+)-independent synaptic vesicle release. Neuron *12*, 1235–1244.

Mizuno, T., Kanazawa, I., and Sakurai, M. (2001). Differential induction of LTP and LTD is not determined solely by instantaneous calcium concentration: an essential involvement of a temporal factor. Eur. J. Neurosci. *14*, 701–708.

Morris, R.G., Garrud, P., Rawlins, J.N., and O'Keefe, J. (1982). Place navigation impaired in rats with hippocampal lesions. Nature *297*, 681–683.

Mulkey, R.M., and Malenka, R.C. (1992). Mechanisms underlying induction of homosynaptic long-term depression in area CA1 of the hippocampus. Neuron *9*, 967–975.

Mulkey, R.M., and Zucker, R.S. (1992). Posttetanic potentiation at the crayfish neuromuscular junction is dependent on both intracellular calcium and sodium ion accumulation. J. Neurosci. *12*, 4327–4336.

Nicoll, D.A., Longoni, S., and Philipson, K.D. (1990). Molecular cloning and functional expression of the cardiac sarcolemmal Na^+-Ca^{2+} exchanger. Science *250*, 562–565.

Nicoll, D.A., Quednau, B.D., Qui, Z., Xia, Y.R., Lusis, A.J., and Philipson, K.D. (1996). Cloning of a third mammalian Na^+-Ca^{2+} exchanger, NCX3. J. Biol. Chem. *271*, 24914–24921.

Phillips, R.G., and LeDoux, J.E. (1992). Differential contribution of amygdala and hippocampus to cued and contextual fear conditioning. Behav. Neurosci. *106*, 274–285.

Podhorna, J., and Brown, R.E. (2002). Strain differences in activity and emotionality do not account for differences in learning and memory performance between C57BL/6 and DBA/2 mice. Genes Brain Behav. *1*, 96–110.

Ranciat-McComb, N.S., Bland, K.S., Huschenbett, J., Ramonda, L., Bechtel, M., Zaidi, A., and Michaelis, M.L. (2000). Antisense oligonucleotide suppression of Na^+/Ca^{2+} exchanger activity in primary neurons from rat brain. Neurosci. Lett. *294*, 13–16.

Regehr, W.G. (1997). Interplay between sodium and calcium dynamics in granule cell presynaptic terminals. Biophys. J. *73*, 2476–2488.

Regehr, W.G., Delaney, K.R., and Tank, D.W. (1994). The role of presynaptic calcium in short-term enhancement at the hippocampal mossy fiber synapse. J. Neurosci. *14*, 523–537.

Reuter, H., and Porzig, H. (1995). Localization and functional significance of the Na^+/Ca^{2+} exchanger in presynaptic boutons of hippocampal cells in culture. Neuron *15*, 1077–1084.

Sakai, K., and Miyazaki, J. (1997). A transgenic mouse line that retains Cre recombinase activity in mature oocytes irrespective of the cre transgene transmission. Biochem. Biophys. Res. Commun. *237*, 318–324.

Sakaue, M., Nakamura, H., Kaneko, I., Kawasaki, Y., Arakawa, N., Hashimoto, H., Koyama, Y., Baba, A., and Matsuda, T. (2000). Na^+-Ca^{2+} exchanger isoforms in rat neuronal preparations: different changes in their expression during postnatal development. Brain Res. *881*, 212–216.

Sanchez-Armass, S., and Blaustein, M.P. (1987). Role of sodium-calcium exchange in regulation of intracellular calcium in nerve terminals. Am. J. Physiol. *252*, C595–C603.

Silva, A.J., Paylor, R., Wehner, J.M., and Tonegawa, S. (1992a). Impaired spatial learning in α-calcium-calmodulin kinase II mutant mice. Science *257*, 206–211.

Silva, A.J., Stevens, C.F., Tonegawa, S., and Wang, Y. (1992b). Deficient hippocampal long-term potentiation in α-calcium-calmodulin kinase II mutant mice. Science *257*, 201–206.

Soderling, T.R., and Derkach, V.A. (2000). Postsynaptic protein phosphorylation and LTP. Trends Neurosci. *23*, 75–80.

Tang, Y.P., Shimizu, E., Dube, G.R., Rampon, C., Kerchner, G.A., Zhuo, M., Liu, G., and Tsien, J.Z. (1999). Genetic enhancement of learning and memory in mice. Nature *401*, 63–69.

Tang, Y.M., Travis, E.R., Wightman, R.M., and Schneider, A.S. (2000). Sodium-calcium exchange affects local calcium signal decay and the rate of exocytotic secretion in single chromaffin cells. J. Neurochem. *74*, 702–710.

Tsien, J.Z., Huerta, P.T., and Tonegawa, S. (1996). The essential role of hippocampal CA1 NMDA receptor-dependent synaptic plasticity in spatial memory. Cell *87*, 1327–1338.

Tsoi, M., Rhee, K.H., Bungard, D., Li, X.F., Lee, S.L., Auer, R.N., and Lytton, J. (1998). Molecular cloning of a novel potassium-dependent sodium-calcium exchanger from rat brain. J. Biol. Chem. *273*, 4155–4162.

Vnek, N., and Rothblat, L.A. (1996). The hippocampus and long-term object memory in the rat. J. Neurosci. *16*, 2780–2787.

Winder, D.G., Mansuy, I.M., Osman, M., Moallem, T.M., and Kandel, E.R. (1998). Genetic and pharmacological evidence for a novel, intermediate phase of long-term potentiation suppressed by calcineurin. Cell *92*, 25–37.

Wojtowicz, J.M., and Atwood, H.L. (1985). Correlation of presynaptic and postsynaptic events during establishment of long-term facilitation at crayfish neuromuscular junction. J. Neurophysiol. *54*, 220–230.

Yang, S.N., Tang, Y.G., and Zucker, R.S. (1999). Selective induction of LTP and LTD by postsynaptic $[Ca^{2+}]_i$ elevation. J. Neurophysiol. *81*, 781–787.

Yu, L., and Colvin, R.A. (1997). Regional differences in expression of transcripts for Na^+/Ca^{2+} exchanger isoforms in rat brain. Brain Res. Mol. Brain Res. *50*, 285–292.

Zucker, R.S. (1999). Calcium- and activity-dependent synaptic plasticity. Curr. Opin. Neurobiol. *9*, 305–313.